引用格式：LIU Qifa, ZHU Lihui, XU Xu, et al. Study on Properties of Fully Etched Bragg Grating Waveguide Filters[J]. Acta Photonica Sinica, 2021, 50(11):1105001
刘启发,朱莉辉,徐许,等.全刻蚀型布拉格波导光栅滤波性能研究[J].光子学报,2021,50(11):1105001

全刻蚀型布拉格波导光栅滤波性能研究

刘启发[1,2],朱莉辉[1],徐许[1],冯柯瑞[1],成谢锋[2]
(1 南京邮电大学 通信与信息工程学院,南京 210003)
(2 南京邮电大学 射频集成与微组装技术国家地方联合工程实验室,南京 210023)

摘 要:提出了一种基于绝缘层上硅波导的全刻蚀布拉格光栅滤波器。该器件可通过对顶部硅的一步刻蚀来实现,其特性使布拉格波长的调谐更加灵敏和有效。仿真研究结果表明,其一阶和三阶光栅的周期对波长调谐系数分别为33 nm/nm和11 nm/nm,光栅刻槽折射率对波长的调谐系数为1 nm/0.006。将光栅脊与刻槽的小折射率差与高阶光栅相结合,可以实现1 550 nm波段更窄带宽的全刻蚀光栅滤波器。

关键词:布拉格光栅;波导滤波器;全刻蚀;有限时域差分仿真;折射率差;波长调谐系数;窄带滤波
中图分类号:O436.1 **文献标识码**:A **doi**:10.3788/gzxb20215011.1105001

Study on Properties of Fully Etched Bragg Grating Waveguide Filters

LIU Qifa[1,2], ZHU Lihui[1], XU Xu[1], FENG Kerui[1], CHENG Xiefeng[2]
(1 *College of Telecommunication and Information Engineering, Nanjing University of Posts and Telecommunications, Nanjing* 210003, *China*)
(2 *National and Local Joint Engineering Laboratory of RF Integration and Micro-Assembly Technology, Nanjing University of Posts and Telecommunications, Nanjing* 210003, *China*)

Abstract: A fully etched Bragg grating filter based on Silicon-On-Insulator(SOI) waveguide is proposed. The full-etched feature makesthe tuning on Bragg wavelength more sensitive and efficient, which can be fabricated by one-step top silicon etching. The simulation results show that the wavelength-period tuning coefficient of 33 nm/nm and 11 nm/nm for the first- and third-order gratings are obtained respectively, groove refractive index tuning has a coefficient of 1 nm/0.006. Combining low refractive index contrast of grating bar and groove with higher grating order, the full-etched grating filter with a narrower bandwidth at 1 550 nm band can be realized.

Key words: Bragg grating; Waveguide filter; Full-etched; FDTD simulation; Refractive index contrast; Wavelength tuning coefficient; Narrow band filtering
OCIS Codes: 050.1950; 130.3120; 130.7408; 230.1480

0 Introduction

Integrated optics is increasingly becoming a topic in hot pursuit in recent years, and has developed rapidly due to its advantages of low time delay, large bandwidth and low loss[1-3]. However, the basic devices of

Foundation item: China Scholarship Council (No.201908320061), Postdoctoral Science Foundation Project of China (No.2018M640507), Open Research Fund of the National and Local Joint Engineering Laboratory of RF Integration and Micro-Assembly Technology (No. KFJJ20180202)

First author (Contact author): LIU Qifa (1981—), male, associate professor, Ph. D. degree, mainly focus on researching in micro-nano optoelectronic devices. Email: liuqf@njupt.edu.cn

Received: Apr.13, 2021; **Accepted**: Jul.4, 2021

integrated optics such as detector, laser, filter[4-8], etc., some are based on III-V compound materials. It is incompatible with the current Complementary Metal-Oxide-Semiconductor (CMOS) process and not conducive to the photoelectric hybrid integration[6-8]. Silicon-On-Insulator (SOI) structure is not only compatible with CMOS process, but also has other obvious advantages such as anti-latch effect, small parasitic capacitance, high integration density, fast speed, simple process, small short channel effect and low power consumption. Therefore, SOI materials have attracted more and more attention[9-11]. Currently, integrated waveguides filters mainly employ the following structures: Mach-Zehnder Interferometer (MZI)[12], micro-ring resonator[13] and grating filter. MZI is based on the principle of interference, which has good filtering characteristics and stability, but its bandwidth is limited by its Free Spectral Range (FSR). Besides, the large size of MZI device limits its applications. Micro-ring has good filtering characteristics, low insertion loss and flexible wavelength adjustment, makes it an excellent on-chip filter. However, lots of problems exist such as small fault tolerance, temperature sensitivity and polarization sensitivity. Bragg waveguide grating can uncouple the optical signal near the resonant wavelength into the mode of reverse transmission. Through periodically etching on the waveguide, different frequency responses can be generated to signals of different wavelengths, thus realizing the filtering function[14]. Due to its convenient bandwidth control, good wavelength stability, simple technology, and no FSR limitation, the Bragg grating has great advantages as a filter.

Driven by the increasing demand of larger capacity optical communication, wavelength selector, optical switch, dense wavelength division multiplexers and optical add-on multiplexers, all need to have the ability of narrow bandwidth to achieve wavelength selection and operation. Meanwhile, high integration, high speed, low energy consumption and low cost are always the core objectives of optical modulator[15]. MURPHY T E et al. first proposed the design of an integrated optical Bragg grating filter based on SOI ridge waveguide in 2001[4]. The filter bandwidth of 0.12 nm was achieved by grating with a length of about 4 mm. This report opened the curtain of designing a SOI based Bragg grating filter. Since then, with the development of integrated optics and the progress of SOI processing technology, waveguide Bragg grating filter has been widely investigated. Different Bragg grating filters based on strip waveguides, such as sampling type[16], chirped type[17-18] and Moire phase shift type[19], have also been proposed. However, much of the reported SOI based filters are based on some complex grating structures such as Moire phase-shifting grating. In addition, most of the grating filters are shallow-etched to ensure a smaller filter bandwidth. Because the control of etching rate and depth has always been a bottleneck, the shallow-etched grating has drawbacks of inconsistent depth or accuracy depth control, which may affect the filter performance.

Here, we proposed SOI based fully etched Bragg grating which can realize the functions of filtering and tunable wave decomposition multiplexing. The design and results of the filter will be discussed both theoretically and by Finite Difference Time Domain Method (FDTD) simulation. Compared with micro-ring resonator, MZI and other narrow-band filters, it is more compact and simple to fabricate. The fully etched structure can avoid the drawbacks of shallow etching. Meantime, by filling materials in grating grooves, the refractive index contrast between grating bar and groove could be reduced. Combining with grating order, the optimized narrow-band filter can be achieved. In addition, through the electro-optical control of the refractive index of groove region, the high-efficiency filter tuning could be obtained due to the fully etched grooves in the waveguide center.

1 Modeling and design principle

The structure of the two-dimensional FDTD simulation model is shown in Fig.1. The structure consists of silicon substrate, 2 μm SiO_2 box layer and 220 nm top silicon layer. Periodical rectangle grooves were etched on the top silicon. Nowadays, the etching technology for 220 nm silicon is very mature. Although it may not guarantee the perfect vertical etching, there is no obvious effect on the final result. So we ignore these subtle errors in the simulation, and use a completely vertical etching angle. The groove is filled with material to adjust the refractive index. The grating period is defined as Λ, total number of grating periods is N. Duty cycle f is defined as the ratio of the grating bar width w to the grating period. The light entering the waveguide grating filter is TE wave, which propagates along the waveguide to the grating region. Detector was put in the waveguide at another end of grating. All boundaries were set as Perfect Boundary Condition (PML), which

absorbs wave to simulate infinite space.

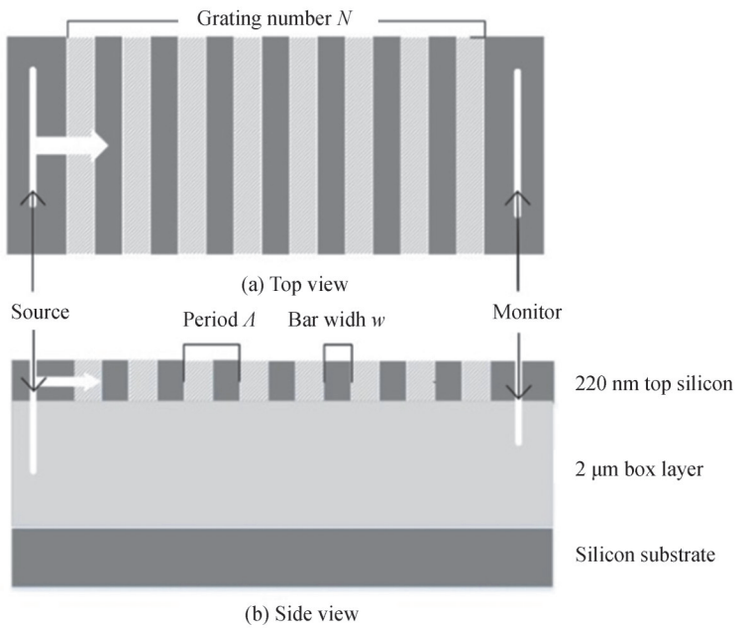

Fig.1 Structure diagram of Bragg grating filter

The Bragg grating is a periodical one-dimensional structure, which forms a certain photonic band gap. The wave falling in the photonic band gap is reflected waves in phase when reflected by the grating, so the overall performance is total wave reflected back. The equation of Bragg filter condition is [20]

$$m\lambda = 2N_{\text{eff}}\Lambda \tag{1}$$

where Λ is the period of grating, λ is the filtering wavelength, N_{eff} is the effective refractive index of grating region, and m is the grating order.

The grating period Λ of the Bragg grating filter can be obtained by Eq. (1). Assuming the refractive index difference between grating bar and groove is very small, the grating period can also be obtained by adding the width of grating bar and the width of grating groove as follows.

The width of bar can be expressed as

$$d_{\text{bar}} = \frac{m\lambda}{4n_2} \tag{2}$$

The width of groove can be expressed as

$$d_{\text{groove}} = \frac{m\lambda}{4n_1} \tag{3}$$

from the bar and the groove width, the duty cycle of grating is as follows.

$$f = \frac{\dfrac{m\lambda}{4n_2}}{\dfrac{m\lambda}{4n_2} + \dfrac{m\lambda}{4n_1}} = \frac{n_1}{n_1 + n_2} \tag{4}$$

The equation of effective refractive index of grating region of TM mode can be approximated as [20-22]

$$N_{\text{eff}}^2 = n_2^2 f + n_1^2(1-f) \tag{5}$$

where n_1 is the refractive index of groove, n_2 is the refractive index of bar. Substituting Eq. (4) into Eq. (5) leads to

$$N_{\text{eff}}^2 = n_2^2 f + n_1^2(1-f) = n_2^2\frac{n_1}{n_2+n_1} + n_1^2\frac{n_2}{n_2+n_1} = n_2 n_1 \tag{6}$$

so the period of grating can be expressed as

$$\Lambda=\frac{m\lambda}{4n_2}+\frac{m\lambda}{4n_1}=\frac{m\lambda(n_2+n_1)}{4n_2n_1}\geqslant\frac{2m\lambda\sqrt{n_2n_1}}{4n_2n_1}=\frac{m\lambda}{2\sqrt{n_2n_1}}=\frac{m\lambda}{2N_{\text{eff}}} \tag{7}$$

The equation of effective refractive index of TE mode can be approximated as

$$\frac{1}{N_{\text{eff}}^2}=\frac{1}{n_2^2}f+\frac{1}{n_1^2}(1-f) \tag{8}$$

substituting Eq. (4) into Eq. (8) leads to

$$\frac{1}{N_{\text{eff}}^2}=\frac{1}{n_2^2}\frac{n_1}{n_2+n_1}+\frac{1}{n_1^2}\frac{n_2}{n_2+n_1}=\frac{(n_2+n_1)^2}{n_2^2n_1^2}-\frac{3}{n_2n_1}\geqslant\frac{1}{n_2n_1} \tag{9}$$

The period in TE mode can be expressed as

$$\Lambda=\frac{m\lambda}{4n_2}+\frac{m\lambda}{4n_1}=\frac{m\lambda(n_2+n_1)}{4n_2n_1}\geqslant\frac{2m\lambda\sqrt{n_2n_1}}{4n_2n_1}=\frac{m\lambda}{2\sqrt{n_2n_1}}=\frac{m\lambda}{2N_{\text{eff}}} \tag{10}$$

When the refractive index of the groove is similar to that of silicon, Eq. (7), Eq. (9) and Eq. (10) can be approximately taken as equal signs. Therefore, no matter in TE mode or TM mode, when the refractive index of the groove is similar to that of silicon, the guiding design of grating period can be obtained by Eq. (1) through approximate analytical calculation of effective refractive index, or the approximate calculation of grating bar and grating groove width by Eq. (2) and Eq. (3).

From the Bragg condition and the equation of the effective refractive index, we can get that the main factors that affect the filtering wavelength are: period, duty cycle, and the refractive index of the groove region, in which period directly affects the filtering wavelength, refractive index and duty cycle affect the effective refractive index of the grating region and then change the filtering wavelength.

2 Results and discussions

2.1 Grating periods number *N*

According to the coupled mode theory[23], the maximum reflectivity of the Bragg grating is as follows

$$R_{\max}=\tanh^2(KL) \tag{11}$$

where K is the coupling coefficient, L is the length of the grating region. The longer the grating region is, the higher the reflectivity will be. However, too many grating numbers will bring additional loss. So N needs to be optimized to achieve the best filtering feature. The calculated results are shown in Fig.2.

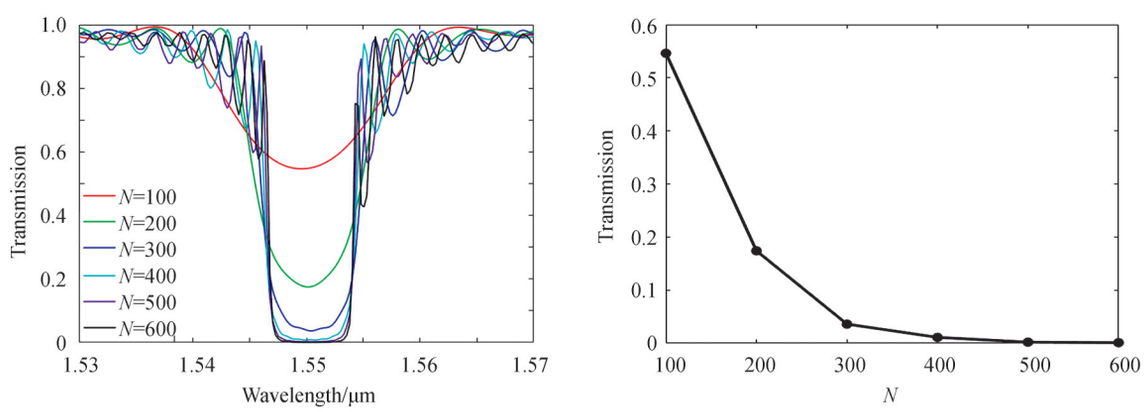

(a) Transmission spectrum at different grating numbers (b) Relationship between transmission and grating numbers

Fig.2 The transmission spectrum of the waveguide gratings with different grating numbers and relationship between transmission and grating numbers

Fig. 2 exhibits the transmission spectrum with grating number from 100 to 600. It can be seen that the transmissivity decreases with the increase of N. When N is 500, the transmissivity of filter wavelength has been reduced to about 0.001. Further increasing the number of gratings will bring unnecessary loss. Therefore, the number of gratings N was set as 500.

2.2 Investigation on filtering bandwidth

There are many factors affect the Bragg bandwidth. According to the coupled mode theory, when the transmissivity is approaching to 0, the Bragg grating bandwidth can be expressed as [23]

$$\Delta\lambda = \frac{2\lambda_B \Lambda}{L}\sqrt{1+\left(\frac{KL}{\pi}\right)^2} \tag{12}$$

where λ_B is the filter resonance wavelength, K is the coupling coefficient, and L is the grating length. The simulation results show that the change of grating length in a small range has no obvious effect on the filter bandwidth. Only when the grating length is increased by a few millimeters, the filter bandwidth will be reduced by a few nanometers. According to the coupled mode theory of high-order Bragg grating, the coupling coefficient K can be expressed as

$$K = \frac{\omega\varepsilon_0 (n_2 - n_1)^2}{16\pi m r} A^2 [\sin(2rh) + 2rh] \tag{13}$$

where ω is the angular frequency of light wave, ε_0 is the dielectric constant in vacuum, h is the height of the grating, m is the grating order and $n_2 - n_1$ is the refractive index difference between grating bar and groove. Therefore, it can be seen that the coupling coefficient is inversely proportional to the grating order and directly proportional to the refractive index difference.

Combining Eq. (12), it can be deduced that the higher grating order or the smaller refractive index difference, the narrower bandwidth. Therefore, we set the refractive index of Si as 3.48, the refractive index of the groove as 3.47 to ensure an enough small refractive index difference. At the same time, we use the third-order Bragg grating filter. In order to verify the feasibility of improving the grating order to reduce the bandwidth. The first-order was also investigated to make a comparison. The parameters of the first-order and third-order Bragg grating are: Λ=226.86 nm, f=0.5 and Λ=680.5 nm, f=0.5, respectively.

Fig. 3 shows the simulated results of transmissivity of the light in the range of 1.53 μm to 1.57 μm after passing through the first-order and third-order gratings. The insets are the field wavelength diagram after filtered by the first-order grating, and the third-order grating, the ordinate is the corresponding filtering wavelength, "y" is the coordinate range corresponding to the side of the grating. On the right are the colors corresponding to different light field intensities. The filter bandwidth of the first-order grating is 6.5 nm, while that of the third-order is 2.1 nm. It can be concluded that the bandwidth of the filter is significantly reduced by

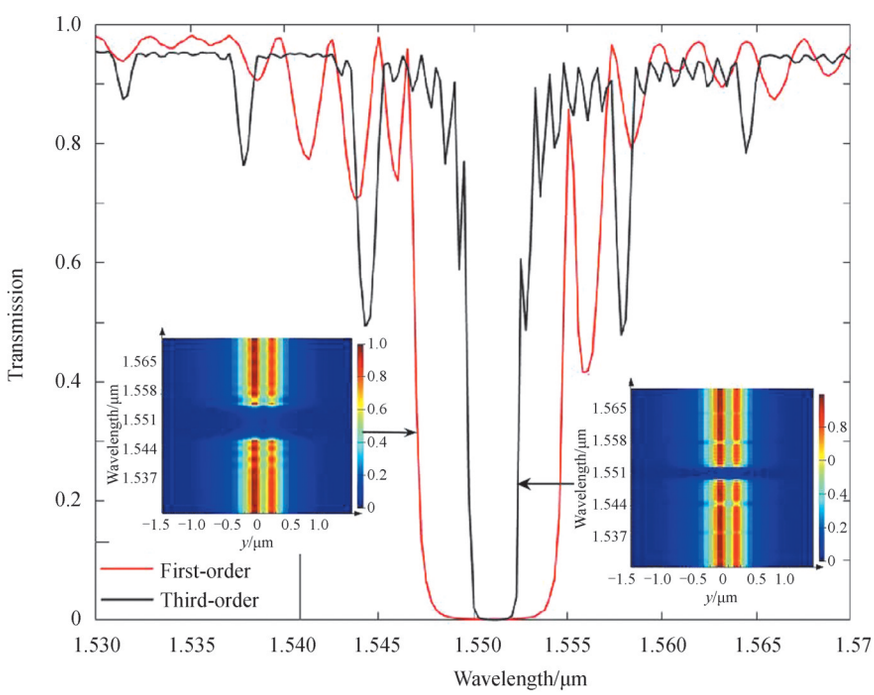

Fig.3 Transmission curves of bandwidth comparison between the first-order and the third-order Bragg grating filters

using higher order grating. The insets show the output field diagram of the waveguide of the first-order and third-order Bragg gratings. The light wave near 1 550 nm fails to pass through the grating, while the light at other bands is successfully transmitted to the waveguide end. The field maps are in good accordance with the transmission lines, and the bandwidth is apparently reduced in the third-order grating.

2.3 Investigation on tunable filtering

2.3.1 *Realization of tunable narrowband filter by period regulation*

According to the Bragg condition (Eq. (1)), when the effective refractive index is fixed, the filter wavelength is changing linear with period. According to the discussion of bandwidth in the previous section, the following parameters was fixed: the refractive index of Si $n_{Si}=3.48$, the refractive index of groove $n_{fill}=3.47$, and the duty cycle $f=0.5$. The period Λ of the first-order grating filter changes from 226.77 nm to 226.95 nm, and the period Λ of the third-order grating filter changes from 680.3 nm to 680.84 nm. The simulated results are shown in Fig.4.

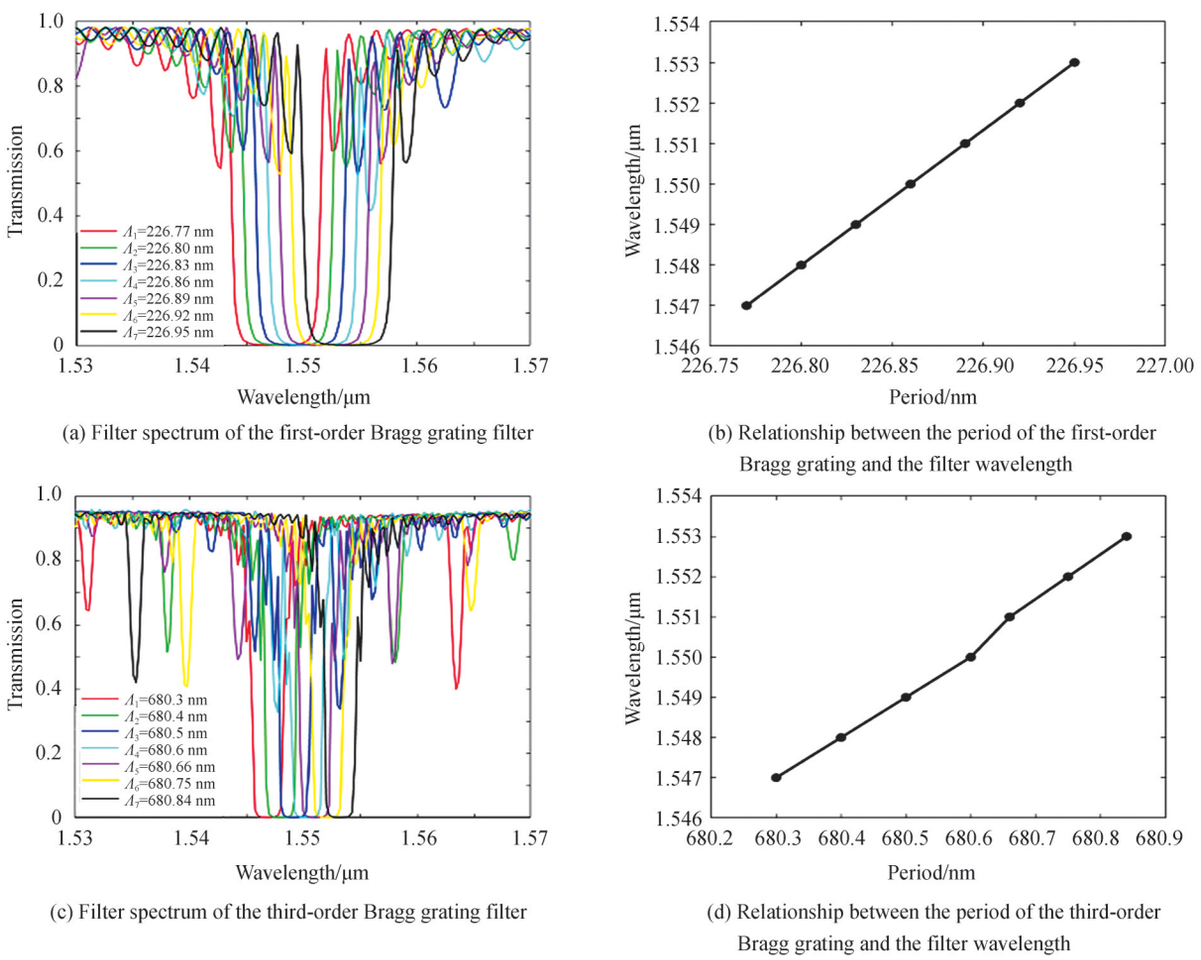

(a) Filter spectrum of the first-order Bragg grating filter

(b) Relationship between the period of the first-order Bragg grating and the filter wavelength

(c) Filter spectrum of the third-order Bragg grating filter

(d) Relationship between the period of the third-order Bragg grating and the filter wavelength

Fig.4 Fixed groove refractive index and grating duty cycle, the filter spectrum changing with grating period of the first-/third-order gratings and the relations of period and filter wavelengths

It can be seen from Figs.4(a) and (c) that, with the increasing of grating period, the corresponding filter wavelength of both the first-order and the third-order Bragg gratings have redshift. It is more obviously reflected in Figs.4(b) and (d), the linear relationship between the filtering wavelength and the period conforms to the Bragg condition. According to the slope equation

$$k=\frac{\lambda_2-\lambda_1}{\Lambda_2-\Lambda_1} \tag{14}$$

It is calculated that the slope of Fig.4(b) is about 33, while the slope of Fig.4(d) is about 11, which represents 1 nanometer change of grating period will bring 33 and 11 nanometer change of filtering wavelength.

It can be concluded that, increasing the grating order reduces the sensitivity of wavelength dependence on period, and the sensitivity of the third-order grating is about one-third of the first-order grating.

In another aspect, the filter bandwidth has been significantly reduced with the increase of grating order. Nevertheless, the side lobes interference has also been increased. This is because the equation of refractive index distribution along the propagation direction in the waveguide grating can be expressed as [24]

$$n_{\mathrm{eff}}(z)=n_0+\delta n_{\mathrm{eff}}(z)\left\{1+v\cos\left[\frac{2\pi}{\Lambda}z+\varphi(z)\right]\right\} \tag{15}$$

where n_0 is the effective index of the waveguide, $\delta n_{\mathrm{eff}}(z)$ is the amplitude change of the index modulation, v is the fringe visibility of the index change, $\varphi(z)$ is the phase shift, and the local index of the grating can be expressed as $\delta n_{\mathrm{eff}}(z)$. The sine variation of effective refractive index is $\delta n_{\mathrm{eff}}(z)v\cos\left[\frac{2\pi}{\Lambda}z+\varphi(z)\right]$. Therefore, the refractive index distribution along the transmission direction can be regarded as the local refractive index plus a sine variation. The amount of change in sine variation is cyclical. Because the grating structure of Bragg grating starts and ends abruptly, not a slow change process, which makes the sine part of the refractive index abruptly change at both ends of the grating, resulting in a lot of side lobes. With the increase of grating order, the grating period increases, the length of grating increases, and the additional loss is increased. Therefore, the transmissivity of the non-resonant wavelength of the high-order grating is lower than that of the first-order grating.

2.3.2 *Realization of tunable narrow band filter with refractive index control*

Combining Eq. (1) and Eq. (8), the effective refractive index can be changed by changing the refractive index of the material in the groove. Then the purpose of adjusting the filtering wavelength can be achieved. In addition, the filter wavelength could be regulated in real-time style by changing the groove refractive index based on the electro-optic or thermo-optic effect. Similarly, here we investigate both the first- and third-order Bragg gratings. The fixed parameters are as follows: the period of the first-order Bragg grating Λ=226.95 nm, the duty cycle f=0.5, the refractive index of the groove n_{fill} changes from 3.428 to 3.47; the period of the third-order Bragg grating Λ=680.9 nm, the duty cycle f=0.5, and the refractive index of the groove n_{fill} changes from 3.428 to 3.47. The results are shown in Fig.5.

From Fig.5, the filter resonance wavelength can be tuned approximately linearly by changing the refractive index of the groove material with a uniform step. With the increase of the refractive index, the filter wavelength changes from 1 547 nm to 1 554 nm. Meanwhile, the slopes of the two lines in Figs.5(b) and (d) are almost the same. It denotes both the first-order and the third-order grating have the same sensitivity. It can be calculated out that the regulation coefficient is 1 nm/0.006, which means the change in refractive index of 0.006 will result in 1 nm shift of the wavelength. However, it can be seen from Fig.5(c) that in the high-order grating, with the increases of the refractive index difference between groove and bar, the side lobes becomes more and more obvious, and the transmissivity at unfiltered wavelength is obviously reduced. As mentioned previously, theside lobes is attributed to abruptly starts and ends of grating, which makes the sine part of the refractive index

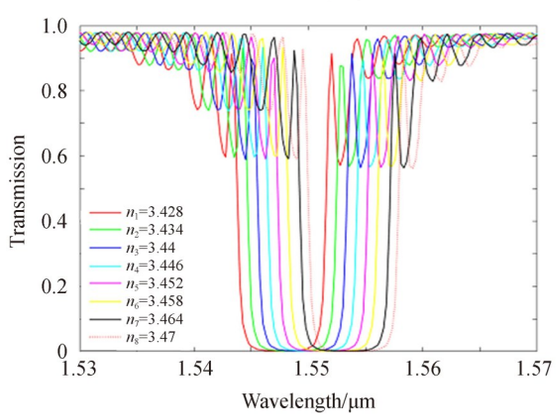

(a) Filter spectrum of the first-order Bragg grating filter

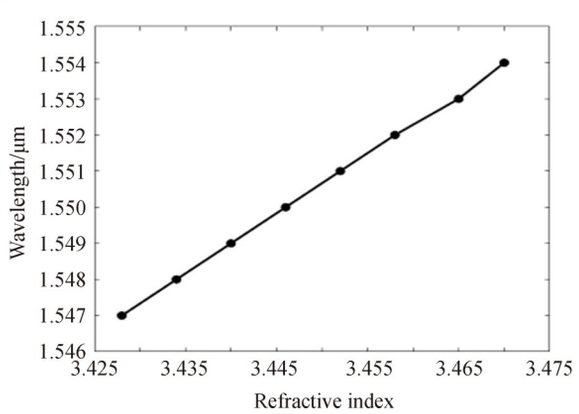

(b) Relationship between the refractive index of the first-order Bragg grating and the filter wavelength

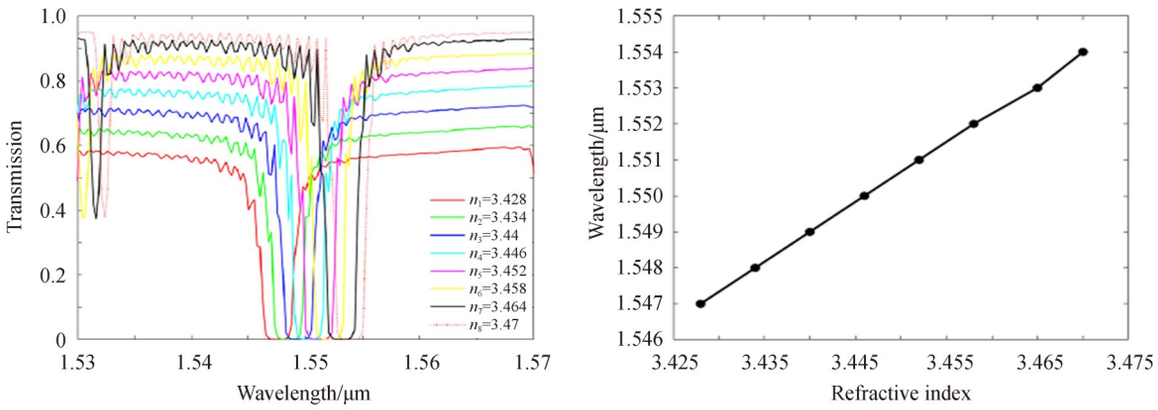

(c) Filter spectrum of the third-order Bragg grating filter

(d) Relationship between the refractive index of the Bragg grating and the filter wavelength

Fig.5 The filter spectrum changing with refractive index of the first-/third- order gratings and the relations of the refractive index and filter wavelengths

abruptly change at both ends of the grating.

According to Eq. (13), if the refractive index difference between bar and groove increases, the coupling coefficient K will increase accordingly. Therefore, according to Eq. (16), the increase of the coupling coefficient K leads to the increase of the reflectivity. Therefore, as the refractive index difference increases, the transmissivity of light of all wavelengths decreases. In addition, a uniform grating can be regarded as a combination of several small uniform gratings whose length is the period of grating. The increase of grating order means the increase of grating period, so that the length of each small uniform grating increases. According to Eq. (16), the reflectivity of light through each small uniform grating increases, plus the additional loss caused by the increase of length. Therefore, in the case of fixed grating period number, when the refractive index difference is the same, the transmissivity of the same wavelength light passing through the third-order grating is smaller than that passing through the first-order grating.

$$R=\frac{|K|^2\sinh^2(rL)}{(\Delta\beta)^2\sinh^2(rL)+|r|^2\cosh^2(rL)} \tag{16}$$

where K is the coupling coefficient, L is the length of the grating, $r^2=|K|^2-\Delta\beta^2$, $\Delta\beta$ is the phase mismatch amount.

Changing the refractive index of the material of groove can achieve real-time adjustment of the filter resonance wavelength. It can be realized by combining the thermal effect of the material with the temperature dependence of the Bragg grating[25]. The temperature dependence of Bragg grating can be determined by the following equation:

$$\frac{\Delta\lambda_B}{\lambda_B}=\frac{\Delta(N_{eff}\Lambda)}{N_{eff}\Lambda}=\left(\frac{1}{\Lambda}\frac{\Lambda}{\partial T}+\frac{1}{N_{eff}}\frac{\partial N_{eff}}{\partial T}\right)\Delta T=(\alpha+\zeta)\Delta T=\beta_T\Delta T \tag{17}$$

where β_T is the thermal sensitivity of the Bragg grating, α is the thermal expansion coefficient of the waveguide, and ζ is the thermal optical coefficient. Therefore, the temperature sensitivity of Bragg grating can be expressed as follows

$$\frac{\Delta\lambda_B}{\Delta T}=\beta_T\lambda_B \tag{18}$$

However, when using thermo-optic effect to change the refractive index of the groove material, it is necessary to consider the strain effect of heating on the thermal expansion and contraction of the grating structure. Therefore, another method can be considered is the electro-optical effect. The refractive index of the material can be changed through the electro-optical effect[26]. In this way, not only the strain effect caused by thermal expansion and contraction can be reduced, but also the electro-optic effect modulation has the advantage of high-speed modulation compared with the thermo-optic effect.

Most of the reported tunable Bragg grating filters are based on thermo-optical and electro-optical effect.

HONG Liang proposed a kind of fiber Bragg grating is with filter wavelength tuning coefficient around 10 pm/K caused by the thermal-optical effect (thermal-expansion coefficient around 10^{-6}/K)[27]. WANG Jihou et al. reported thermo-optic tunable chirped waveguide Bragg gratings using organic-inorganic hybrid PMMA materials has 200 pm/K sensitivity[28]. Some other reports utilizing thermal-expansion effect is with regulation coefficient of around 2 nm/mW[29-30] and 0.2 nm/°C[31-32]. YUAN Yao investigate Lithium Niobate Bragg grating using electro-optical effect with tunning sensitivity larger than 4.6 pm/V[33]. And other reports using electro-optical effect with around 4 pm/V tunning coefficient[34-35].

In addition, from Fig.5(c), we find that when the refractive index difference between the filled medium and silicon is large, the loss of non-resonant wavelength in the third-order grating filter is larger than expected. We consider the reason to be the influence of grating length. The simulation in Fig.5(c) is carried out under the condition of the same number of gratings, so the length of the third-order grating is improved compared with that of the first-order grating. In order to verify the conjecture, simulations with consistent grating length were performed. Fix the following parameters: the refractive index of Si $n_{Si}=3.48$, In order to get a more obvious effect, we set the refractive index of the filled medium as $n_{fill}=3.428$, duty cycle $f=0.5$, cycle $\Lambda=680.3$ nm. The simulation results are shown in Fig.6. When the grating length of the third-order filter is reduced to the same as that of the first-order grating, the transmission of the non-resonant wavelength is significantly improved, from the original 50% to 60% to more than 80%, and the filter loss is significantly reduced. Therefore, we can conclude that the loss of non-resonant wavelength is mostly caused by the grating length. Meantime, when the grating length of the third-order grating filter is the same as that of the first-order grating filter, the transmittance of the resonant wavelength also increases significantly compared with that of the first-order grating filter. According to the coupling coefficient equation, this is because when the refractive index difference between the filled medium and silicon is fixed, the order of the grating increases, which leads to the decrease of the coupling coefficient and the reflectivity.

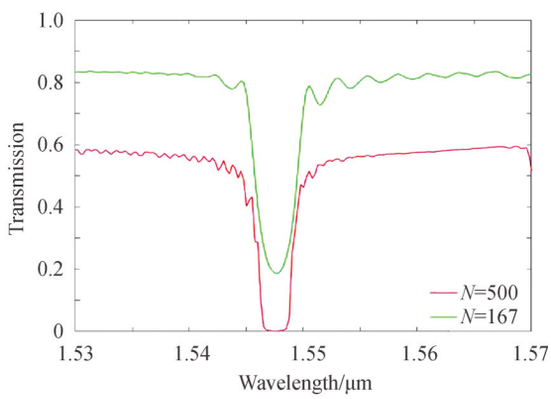

Fig.6 Comparison of filtering spectral lines when the number of gratings of the third-order grating is 500 and 167

2.3.3 *Discussion on adjustable filtering by duty cycle controlling*

According to the equation of effective refractive index (Eq. (8)), the effective refractive index is not only related to the refractive index of the materials, but also related to the duty cycle. So the filtering wavelength can be adjusted by changing the duty cycle theoretically. The simulations with the following parameters was carried out: the number of gratings $N=500$, the refractive index of Si $n_{Si}=3.48$, the refractive index of groove $n_{fill}=3.428$, the period of the Bragg grating $\Lambda=227$ nm, The duty cycle f changes from 0.2 to 0.8. The simulated results are shown in Fig.7.

With the increase of duty cycle, the filtering wavelength has a significant red shift, from 1 545 nm to 1 554 nm. We attribute the reason to the increasing of effective refractive index, which explained by Eq. (8). So the filtering wavelength increases accordingly. From Fig.7, except for duty cycle of 0.5, the transmittance of the resonant wavelength under other duty cycles increases to a certain value, and the filtering efficiency of the resonant wavelength decreases. Besides, not all duty cycle cases will get better transmittance spectral. The filtering spectral diagram under $f=0.4$ is shown in Fig. 8. The ordinate is the corresponding filtering

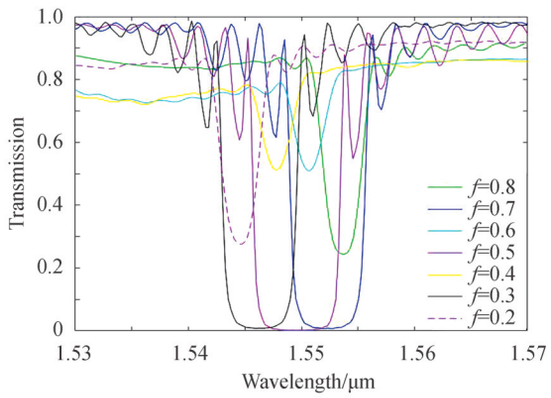

Fig.7 The relationship between wavelength and grating transmittance under different duty cycle

wavelength, "y" is the coordinate range corresponding to the side of the grating. On the right are the colors corresponding to different light field intensities.

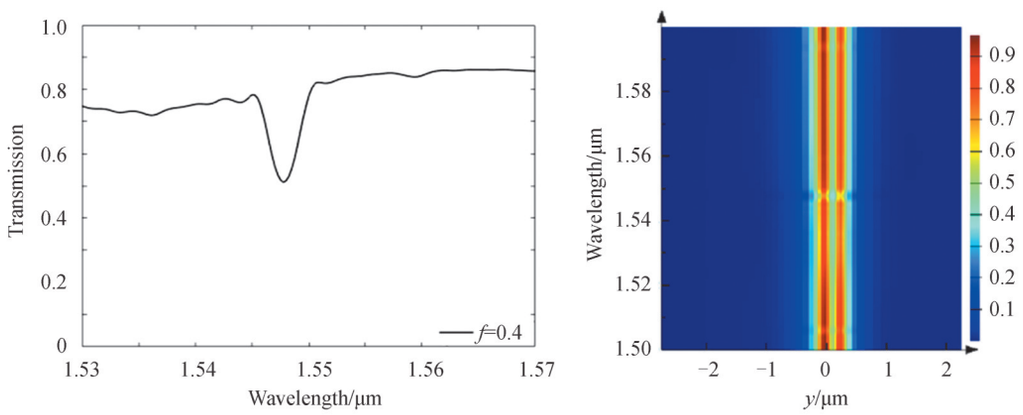

(a) The filtered spectrum with 0.4 duty cycle (b) The filtered light field with 0.4 duty cycle

Fig. 8 Fix the period of grating and refractive index of filled medium, the filtered spectrum and filtered light field with 0.4 duty cycle

In this situation, the transmittance of the resonant wavelength is 50%. From the field distribution (Fig.8 (b)), 1 550 nm wavelength is not completely filtered, and a large part of the light passes through the grating region. This indicates that the grating filter can not efficiently filter the signal of the resonant wavelength in this case. At the same time, the transmittance of the light with non-resonant wavelength decreases obviously. The lowest point is 72%, indicates a serious loss. Therefore, for non-real-time adjustment of filter wavelength, it is not ideal to adjust the filter wavelength by changing the duty cycle.

The essence of adjusting the filter wavelength by duty cycle is to change the effective refractive index of the grating. The range of adjustment depends on the refractive index of the filled medium and the refractive index of Si. According to the formula of effective refractive index, the minimum effective refractive index of the grating is the refractive index of the filled medium, and the maximum is the refractive index of Si, which corresponds to the duty cycle of 0 and 1 respectively. However, when the refractive index of the two materials is similar, the influence of duty cycle change on the effective refractive index is very limited, so it is impossible to realize the efficient adjustment of the wavelength.

3 Conclusion

We proposed a kind of fully etched Bragg waveguide grating filter. The filter properties correlated to grating period and refractive index were mainly explored theoretically and by simulation. In principle, a very low refractive index contrast grating bar and groove should be designed for a narrow band filter. And higher grating order is beneficial to realize narrower band filter. The reflected wavelength is linearly controlled by grating

period with a sensitive regulation coefficient, and also linearly tuned by refractive index of groove material. The change of the period can adjust the filter wavelength with regulation coefficient of 33 nm/nm and 11 nm/nm for first-order grating and third-order grating, respectively. The refractive index of the groove can tune the filter wavelength with 1 nm/0.006 coefficient. The filter bandwidth is fundamentally limited by the high refractive index of silicon and the volume of etched region. If the waveguide with lower refractive index than silicon or the method of edge-etched waveguide were used, the filter with narrower band or excellent regulation performance could be realized.

References

[1] MILLER S E. Integrated optics: An introduction[J]. Bell System Technical Journal, 1969, 48(7):2059-2069.

[2] ARAKAWA Y, NAKAMURA T, URINO Y, et al. Silicon photonics for next generation system integration platform[J]. IEEE Communications Magazine, 2013, 51(3): 72-77.

[3] SOREF R. The past, present, and future of silicon photonics[J]. IEEE Journal of Selected Topics in Quantum Electronics, 2007, 12(6):1678-1687.

[4] MURPHY T E, HASTINGS J T, SMITH H I. Fabrication and characterization of narrow-band Bragg-reflection filters in silicon-on-insulator ridge waveguides[J]. Journal of Lightwave Technology, 2001, 19(12): 1938-1942.

[5] QIU H, JIANG G, HU T, et al. FSR-free add-drop filter based on silicon grating-assisted contradirectional couplers[J]. Optics Letters, 2013, 38(1): 1-3.

[6] PAINTER O J, HUSAIN A, SCHERER A, et al. Room temperature photonic crystal defect lasers at near-infrared wavelengths in InGaAsP[J]. Journal of Lightwave Technology, 1999, 17(11): 2082-2088.

[7] PARK H, KIM S, KWON S, et al. Electrically driven single-cell photonic crystal laser[J]. Science, 2004, 305(5689): 1444-1447.

[8] REN Gang, ZHENG Wanhua, ZHANG Yejin, et al. Room-temperature photonic crystal laser in H3 cavity on InGaAsP/InP slab[J]. Chinese Physics Letters, 2008, 25(3): 981-984.

[9] PARK H, KOCH B R, NORBERG E J, et al. Heterogeneous integration of silicon photonic devices and integrated circuits [C]. Lasers & Electro-optics Pacific Rim. IEEE, 2015.

[10] PORZI C, SERAFINO G, VELHA P, et al. Integrated SOI high-order phase-shifted bragg grating for microwave photonics signal processing[J]. Journal of Lightwave Technology, 2017, 35(20): 4479-4487.

[11] JIANG Weijun, XU Lu, LIU Yifan, et al. Optical filter switchable between bandstop and bandpass responses in SOI wafer [J]. IEEE Photonics Technology Letters, 2020, 32(17):1.

[12] LUO Zhichao, LUO Aiping, XU Wencheng. Polarization-controlled tunable all-fiber comb filter based on a modified dual-pass Mach - Zehnder interferometer[J]. IEEE Photonics Technology Letters, 2009, 21(15): 1066-1068.

[13] CHENG Jun, YAN Nan. Three-step lithography to the fabrication of vertically coupled micro-ring resonators in amorphous silicon-on-insulator[J]. Chinese Optics Letters, 2015, 13(8): 082201.

[14] ROSENBLATT D, SHARON A, FRIESEM A A. Resonant grating waveguide structures [J]. IEEE Journal of Quantum Electronics, 1997, 33(11): 2038-2059.

[15] MELIKYAN A, ALLOATTI L, MUSLIJA A, et al. High-speed plasmonic phase modulators[J]. Nature Photonics, 2014, 8(3): 229-233.

[16] HAO Lijun, SHI Yuechun, XIAO Rulei, et al. Study on sampled waveguide grating with antisymmetric periodic structure [J]. Optics Express, 2015, 23(12): 15784-15791.

[17] OKAYAMA H, ONAWA Y, SHIMURA D, et al. Si waveguide polarisation rotation chirped Bragg grating [J]. Electronics Letters, 2016, 53(2): 96-98.

[18] FENG Wenbin, GU Zhengtian. Ultra-broadband optical filter based on chirped long-period fiber grating and PMTP[J]. IEEE Photonics Technology Letters, 2018, 30(15): 1361-1363.

[19] MIN Rui, MARQUES C, BANG o, et al. Moire phase-shifted fiber Bragg gratings in polymer optical fibers[J]. Optical Fiber Technology, 2018, 41: 78-81.

[20] KANG Jian , CHENG Zhenzhou, ZHOU Wen, et al. Focusing subwavelength grating coupler for mid-infrared suspended membrane germanium waveguides[J]. Optics Letters, 2017, 42(11):2094-2097.

[21] CHEN Xia, LI Chao, CHRISTY K Y, et al. Apodized waveguide grating couplers for efficient coupling to optical fibers [J]. IEEE Photonics Technology Letters, 2010, 22(15): 1156-1158.

[22] MARCHETTI R, LACAVA C, CARROLL L, et al. Coupling strategies for silicon photonics integrated chips [J]. Photonics Research, 2019, 7(2): 201-239.

[23] PIERCE J R. Coupling of modes of propagation[J]. Journal of Applied Physics, 1954, 25(2): 179-183.

[24] ERDOGAN T. Fiber grating spectra[J]. Journal of Lightwave Technology, 1997, 15(8): 1277-1294.

[25] MOHAMMED A Z, ABASS A K, IBRAHIM S K. Design and analysis of fiber Bragg grating tunable filter utilizing

thermal technique[C]. 4th Electronic and Green Materials International Conference 2018 (EGM 2018), 2018.
[26] YUAN, Yao, LIU Haifeng, XUE Lifang, et al. Design of lithium niobate phase-shifted Bragg grating for electro-optically tunable ultra-narrow bandwidth filtering[J]. Applied Optics, 2019, 58(25): 6770-6774.
[27] HONG Liang, KANG Ying, DI Wang, et al. All-fiber narrow-bandwidth rectangular optical filter with reconfigurable bandwidth and tunable center wavelength[J]. Optics Express, 2021, 29(8): 11739-11749.
[28] WANG Jihou, CHAO Liang, GUAN Shang, et al. Metal-print-defining thermo-optic tunable chirped waveguide Bragg gratings using organic-inorganic hybrid PMMA materials[J]. Optical Materials Express, 2018, 8(7): 1870-1881.
[29] DONG Po, QIAN Wei, LIANG Hong, et al. Thermally tunable silicon racetrack resonators with ultralow tuning power [J]. Optics Express, 2010, 18: 20298-20304.
[30] ZHANG Ziyang, NOVO A M, LIU Dongliang, et al. Compact and tunable silicon nitride Bragg grating filters in polymer [J]. Optics Communications, 2014, 321: 23-27.
[31] TIAN Liang, WANG Fei, WU Yuanda, et al. Polymer/silica hybrid integration add-drop filter based on grating-assisted contradirectional coupler[J]. Optics Letters, 2018, 43: 2348-2351.
[32] WANG Jihou, CHEN Changming, WANG Chunxue, et al. Metal-printing defined thermo-optic tunable sampled apodized waveguide grating wavelength filter based on low loss fluorinated polymer material[J]. Applied Sciences, 2020, 10: 167.
[33] YAO Yuan, LIU Haifeng, XUE Lifang, et al. Design of lithium niobate phase-shifted Bragg grating for electro-optically tunable ultra-narrow bandwidth filtering[J]. Applied Optics, 2019, 58(25): 6770-6774.
[34] ZHANG Weifeng, EHTESHAMI N, LIU Weilin, et al. Silicon-based on-chip electrically tunable sidewall Bragg grating Fabry-Perot filter[J]. Optics Letters, 2015, 40: 3153-3156.
[35] WANG Min, XU Yingxin, FANG Zhiwei, et al. On-chip electro-optic tuning of a lithium niobate microresonator with integrate in-plane microelectrodes[J]. Optics Express, 2017, 25: 124-129.